

## Supporting Information

### Unlocking the Access to Natural Identical Vanillin *via* Isoeugenol Ozonation: *in-situ* ATR-IR Monitoring and Safety Evaluation

Yun Zhao<sup>a,b\*</sup>, Tingfei Li<sup>a</sup>, SiSi Xie<sup>a</sup>, Pingyi Zhang<sup>a</sup>, Haifang Mao<sup>a,b\*</sup>

<sup>a</sup>Shanghai Institute of Technology, 100 Haiquan Road, Shanghai, 201418, China.

<sup>b</sup>Shanghai Research Institute of Fragrance & Flavor Industry, 480 Nanning Road, Shanghai, 200232

Corresponding author's email: zhaoyun@sit.edu.cn (Yun Zhao); mhf@sit.edu.cn (Haifang Mao)

#### 1 Experimental Sections

##### ESI 1: HPLC analysis for isoeugenol and vanillin

All the experimental conditions for HPLC tests were the same during the whole work.

Chromatographic column: C18 column (4.6 mm×250 mm, 5 μm)

Column temperature: 298.15 K

Detection wavelength: 232 nm

Injection volume: 10 μL

Flow rate: 1.0 mL/min

Mobile phase:

A — acetonitrile (HPLC);

B — distilled water (containing 0.1% phosphoric acid);

Gradient elution method was adopted (see the table below):

**HPLC mobile phase gradient**

Time /min	A%	B%
0	30	70
8	50	50
13	90	10
14	30	70
20	30	70

External standard curve method was used for isoeugenol and vanillin quantification.

**Establishment of isoeugenol standard curve.** Used mobile phase ( $V_{\text{acetonitrile}}: V_{\text{water}} = 30\%:70\%$ ) to prepare a series of isoeugenol standard solutions with concentrations of 0.04106 mg/mL, 0.1232 mg/mL, 0.2053 mg/mL, 0.2874 mg/mL and 0.4106 mg/mL. The standard solutions were analyzed with the above HPLC analysis method. The retention time for isoeugenol was 13.142 min. Isoeugenol standard curve was obtained by plotting a curve of  $A \sim c$ , and the coefficient of determination  $R^2$  was 0.9997 (**Figure S1a**).

**Establishment of vanillin standard curve.** The standard curve for vanillin was obtained in a similar way. The concentrations for vanillin standard solutions were 0.04210 mg/mL, 0.08416 mg/mL, 0.1262 mg/mL, 0.1683 mg/mL and 0.2104 mg/mL. The retention time for vanillin was 6.096 min. The coefficient of determination  $R^2$  for vanillin standard curve was 0.9995 (**Figure S1b**).

### **ESI 2: Establishment of the mid-infrared quantification model for isoeugenol and vanillin to guide the optimization of experimental conditions**

The characteristic absorption peaks for vanillin and isoeugenol were identified by measuring the infrared spectra of the pure standards with solvent system (methanol-H<sub>2</sub>O) as the reference. As shown in **Figure S2** and **Table S1**, due to the close structure, the infrared spectra for isoeugenol and vanillin was quite similar. However, it was still possible to select the unperturbed 1674 cm<sup>-1</sup> as the characteristic peak for vanillin (corresponding to the stretching vibration of C=O bond of vanillin aldehyde group) and 966 cm<sup>-1</sup> as the characteristic peak for isoeugenol (corresponding to the stretching vibration of C=C double bond (*trans*-) of isoeugenol side chain). The interference of bending mode vibration of water, which absorbed at 1634 cm<sup>-1</sup> could be well eliminated in the present work.

A series of standard solutions of vanillin and isoeugenol with different concentrations were prepared (calibration set), in which the concentration range of isoeugenol was 0-230 mg/mL and that of vanillin was 0-200 mg/mL. Collected the infrared absorption spectra for each standard solution and their contents were accurately quantified by the HPLC method described in **ESI 1**. Linked the the IR absorbance at the characteristic peak of isoeugenol and vanillin with their concentration (converted to mass percentage concentration) and established the *in-situ* mid-infrared quantification model with the help of ICQuant Model (Mettler software) by a univariate linear regression model. Typically, the abscissa was the actual value measured by HPLC, and the ordinate was the predicted value by IR quantification model. An independent test set (validation set) was used to verify each model's predictive accuracy. The determination coefficient of isoeugenol and vanillin infrared model was 0.9922 and 0.9957, respectively, indicating that the infrared quantitative model could predict isoeugenol and vanillin concentration precisely, which was suitable for the *in-situ* quantification during isoeugenol ozonation process (**Figure S3**).

### **ESI 3: Procedure for Safety evaluation**

In a typical experiment, 20 g isoeugenol, 170 mL methanol and 30 mL water were added in sequence into the 1000 mL glass reaction kettle of RC1e. The temperature sensor and calibration heater were inserted below the liquid level. The stirring speed was set to 300 rpm and the reaction temperature was set to 263.15 K ( $\pm 0.3$  K). After the temperature was stable, continued to stirring for another 10 min. The specific heat capacity  $C_{p1}$  (J/g•K) and the comprehensive heat transfer coefficients  $U_1$  and  $U_2$  (W/K•m<sup>2</sup>) of the system were measured before the reaction began. The system was maintained at 263.15 K for 90 min in an ozone atmosphere. Used

the established *in-situ* ATR-IR system to monitor the reaction and stopped the reaction when the characteristic absorption peak for isoeugenol disappeared. The specific heat capacity  $C_{p2}$  (J/g•K) and the comprehensive heat transfer coefficients  $U_3$  and  $U_4$  (W/K•m<sup>2</sup>) of the system were measured at the end of reaction. Finally, the reaction kettle was heated to the room temperature, the product was released from the bottom of the reaction kettle and the accessories and reaction kettle were thoroughly cleaned.

#### ESI 4: Procedure for solubility study of vanillin in methanol-water system

Since isoeugenol was a liquid and could be completely dissolve in methanol-water solvent, the saturated solubility of vanillin was investigated in mixed solvents of methanol and water with different volume ratios. The solubility tests were conducted at 258.15 K with the following procedures.

Firstly, opened the constant temperature circulating water bath and set it to the predetermined temperature of 258.15 K. Weighed 30 g of vanillin and grounded them into powder, then added 100 g of mixed solvent and sealed the reactor with rubber plug. Ultrasound the solution for 30 min to speed up the dissolution. Connected the constant temperature circulating water bath, opened the circulating water, turned on the magnetic stirring and started timing. Holding the solution for 12 h at constant temperature, then turned off the magnetic stirring, and kept warm for 1-2 h. The supernatant was taken and the vanillin content was measured by HPLC.

The molar fraction solubility of vanillin in a methanol-water solvent can be described using equation 1<sup>1</sup>.

$$x_1 = \frac{m_1/M_1}{m_1/M_1 + m_2/M_2 + m_3/M_3} \quad (\text{equation S-1})$$

Where,  $m_1$ ,  $m_2$  and  $m_3$  represent the mass of vanillin, methanol and water respectively.  $M_1$ ,  $M_2$  and  $M_3$  represent the molar mass of vanillin, methanol and water, respectively.

Noticed that the syringes and HPLC needle filters needed to be preheated at 283.15 K higher than the solubility test temperature (258.15 K) to prevent vanillin from crystallizing during sampling. Experimental results were shown in **Table S3**.

Using the data in Table S3 to determine the appropriate concentration for isoeugenol during the whole experiment.

In the methanol-water system, the higher the water content, the lower the vanillin solubility. Therefore, the molar fraction solubility of vanillin in methanol-water (75%:25%, volume ratio) was used to determine the upper limit concentration of vanillin and isoeugenol. Fixed the total solvent volume at 150 mL, where the water volume  $V_2$  was 37.5 mL and methanol volume  $V_3$  was 112.5 mL.

Since  $x_1=0.0244$ ,

$$x_1 = \frac{m_1/M_1}{m_1/M_1 + m_2/M_2 + m_3/M_3}$$

$$x_1 = \frac{m_1/M_1}{m_1/M_1 + \rho_2 V_2/M_2 + \rho_3 V_3/M_3}$$

$$0.0244 = \frac{m_1/152.15}{m_1/152.15 + 37.5/18 + 0.8 \times 112.5/32}$$

Therefore, the amount of vanillin  $m_1$  was calculated to be 18.61 g, indicating that the vanillin concentration should not exceed 124 mg/mL.

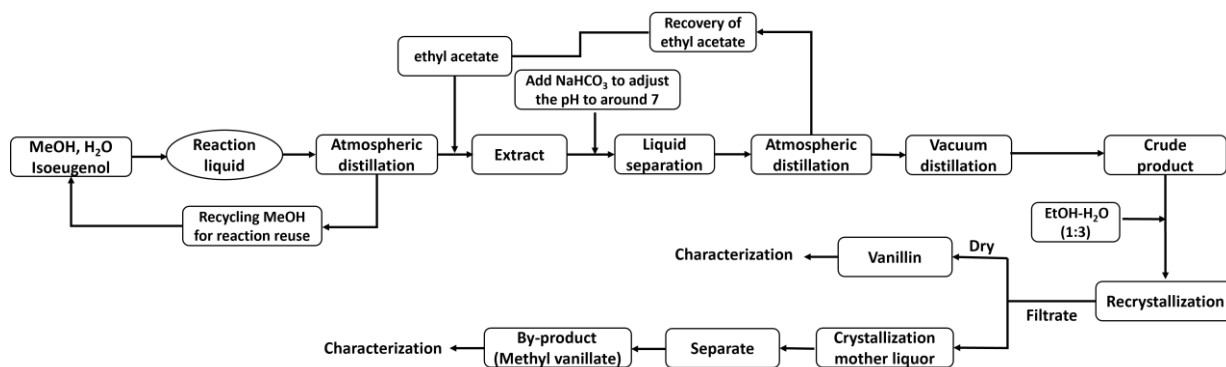
From the chemical equation, 1 mol isoeugenol theoretically produces 1 mol vanillin. Thus, for a 150 mL methanol-water solvent system, isoeugenol concentration should be less than 133.8 mg/mL.

In all the optimization experiments in this work, isoeugenol concentrations were designed below this concentration.

Procedure for solubility study of vanillin and isoeugenol in pure water system was similar just by replacing the solvent of methanol-H<sub>2</sub>O with pure water. Besides, the temperature was adjusted to 278.15 K to prevent water from freezing.

### ESI 5: Procedure for methanol recycling and production separation

Methanol was recycled according to the following procedure: Methanol was recycled through atmospheric distillation, achieving a recovery rate of above 99%. The recycled methanol was then collected for reuse in subsequent reactions. Vanillin crude product was obtained after ethyl acetate extraction (50 mL EA each time, three times), alkaline washing (NaHCO<sub>3</sub> aq.), atmospheric and vacuum distillation. The crude product was recrystallized with EtOH/H<sub>2</sub>O (mass ratio: 1:3) and purified vanillin product was obtained after filtration and drying. The crude product was recrystallized with EtOH/H<sub>2</sub>O (mass ratio: 1:3) and purified vanillin product was obtained after filtration and drying.



Scheme S1. Procedure for solvent recovery and product separation.

## 2 Supporting Figures and Tables

Figure S1: HPLC External Standard Curve for Isoeugenol and Vanillin.

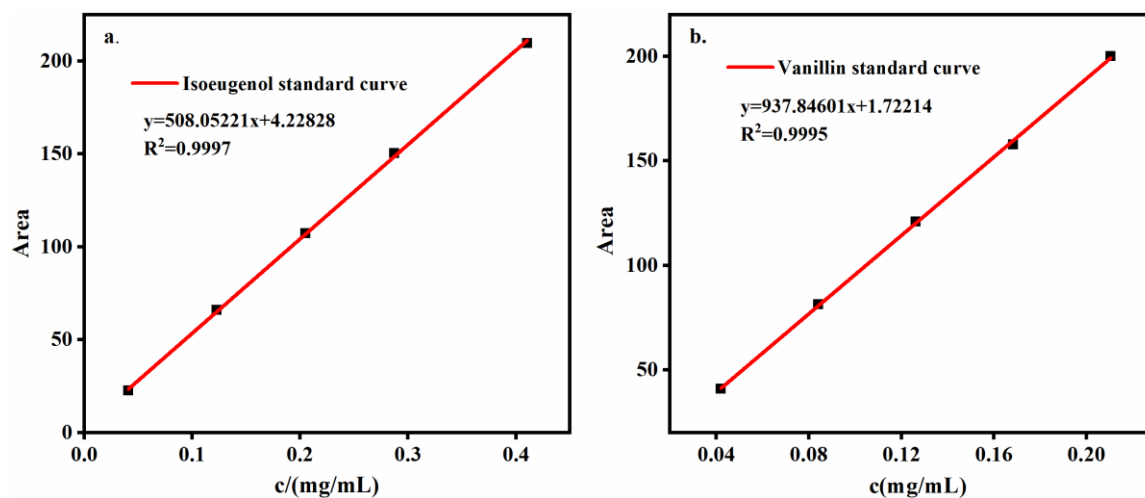


Figure S1. HPLC external standard quantitative curve for (a) isoeugenol and (b) vanillin.

Figure S2: Mid-infrared spectra for isoeugenol, vanillin and the blank.

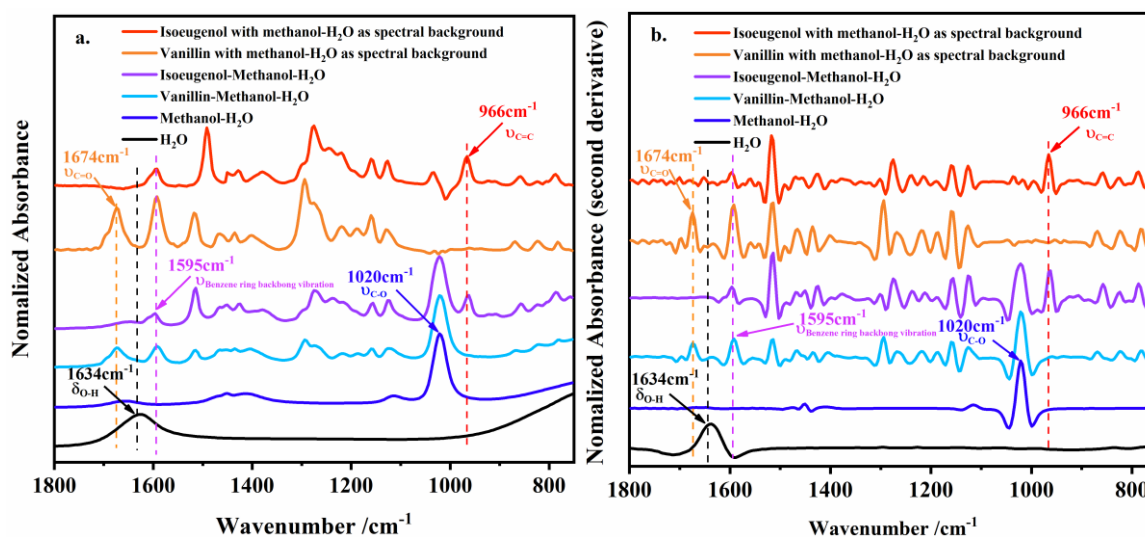


Figure S2. (a) Mid- infrared spectra of vanillin, isoeugenol, reference spectrum (methanol- $\text{H}_2\text{O}$ ),  $\text{H}_2\text{O}$ , vanillin minus reference spectrum and isoeugenol minus reference spectrum; (b) The corresponding second-order derivative spectra for (a). Vanillin or isoeugenol standard was dissolved in methanol- $\text{H}_2\text{O}$ .

Figure S3: Mid-infrared quantitative model for isoeugenol and vanillin.

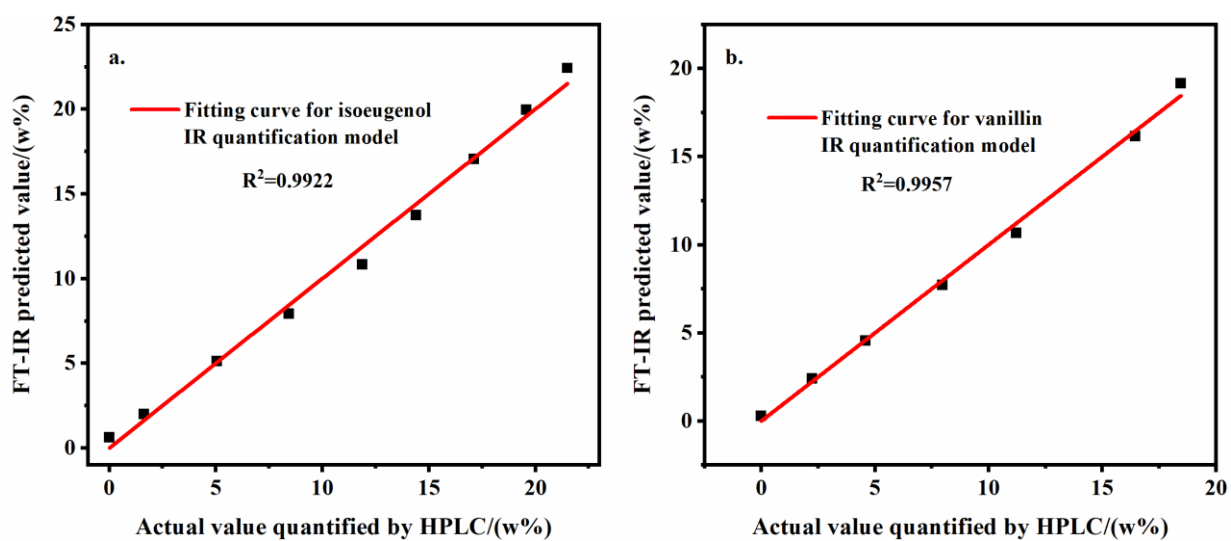


Figure S3. Mid-infrared quantitative model for (a) isoeugenol and (b) vanillin.

Figure S4: *In-situ* ATR-IR spectra during the conversion of isoeugenol (second-order derivative spectra).

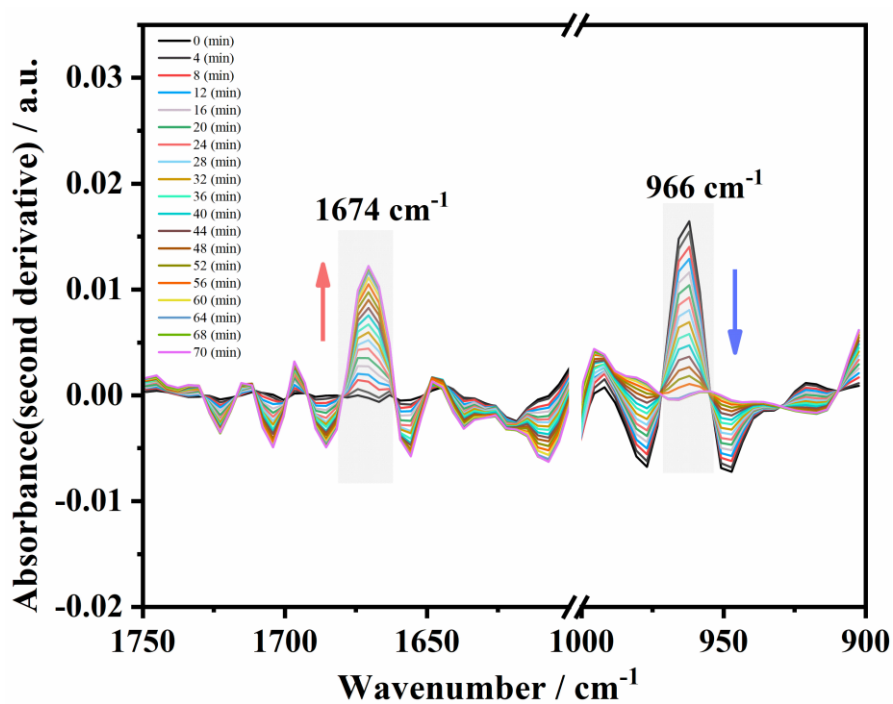


Figure S4. *in-situ* ATR-IR spectra during the conversion of isoeugenol (second-order derivative spectra).

Figure S5: HPLC graph of the reaction system at 60 min (a) and 70 min (b).

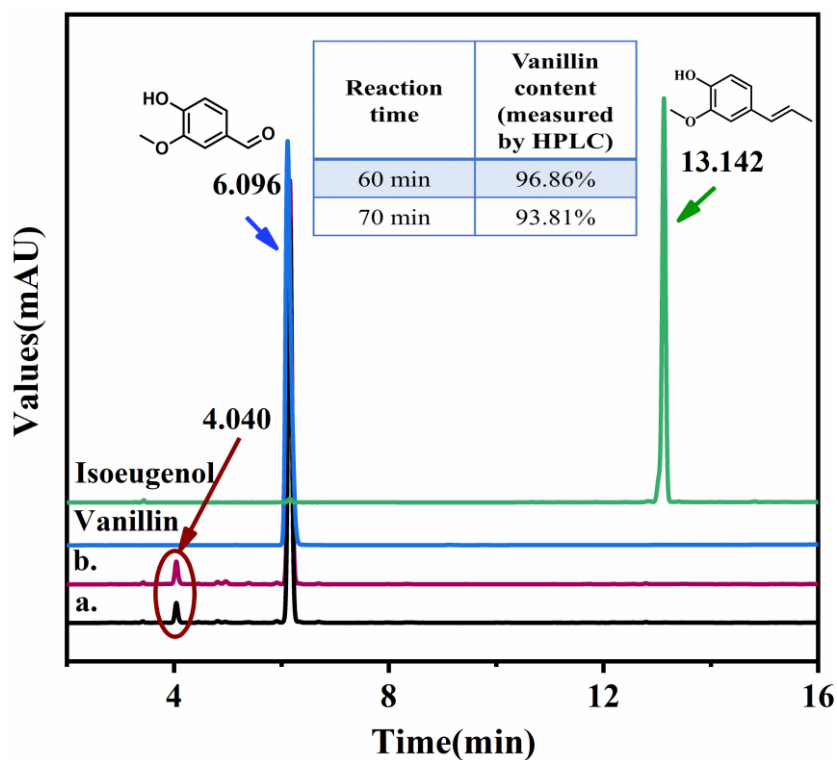


Figure S5. HPLC graph of vanillin (blue curve), isoeugenol standards (green curve) and the reaction system at 60 min (a) and 70 min (b).

Figure S6: HPLC graphs of the reaction system at 268.15 K to 258.15 K.

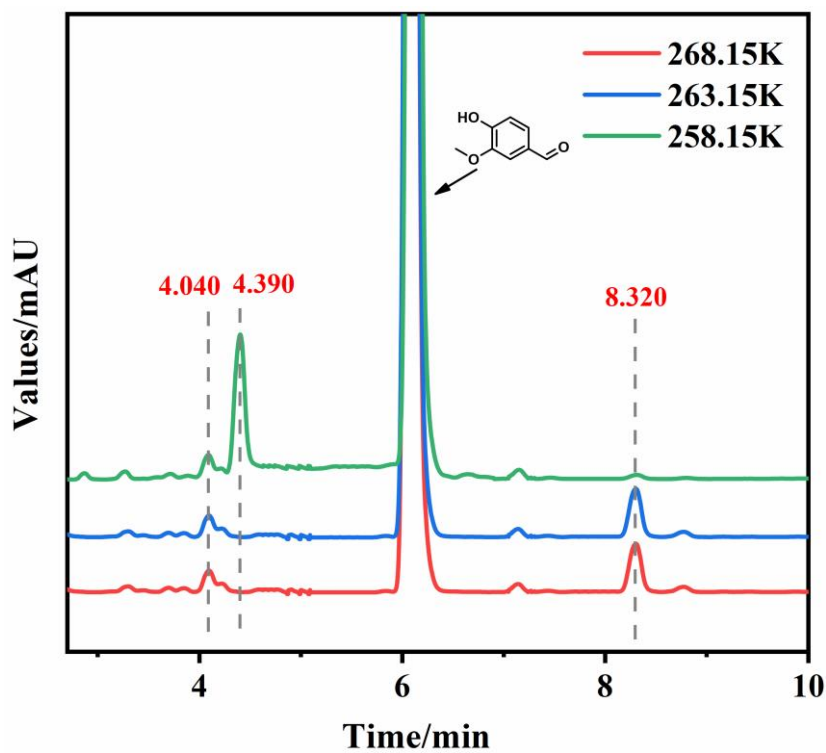


Figure S6. HPLC graphs of the reaction system at 268.15 K to 258.15 K.

Figure S7: Recyclability test of methanol

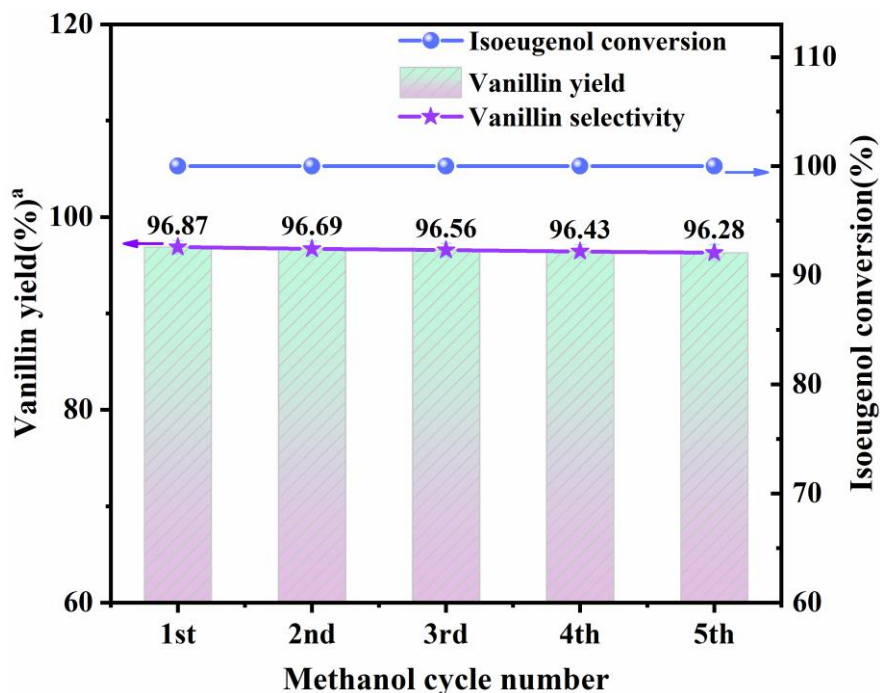


Figure S7. Recyclability test of methanol, Experimental conditions: Isoeugenol concentration: 100 mg/mL,

$V_{\text{methanol}}: V_{\text{H}_2\text{O}}=85:15$ , Reaction temperature: 263.15 K, Gas flux: 1.6 L/min.

<sup>a</sup> herein, the vanillin yield refers to the apparent yield calculated directly from ATR-FTIR quantification model based on the absorbance at the peak of  $1674 \text{ cm}^{-1}$ .

Figure S8: pH variation of the reaction system during isoeugenol ozonation.

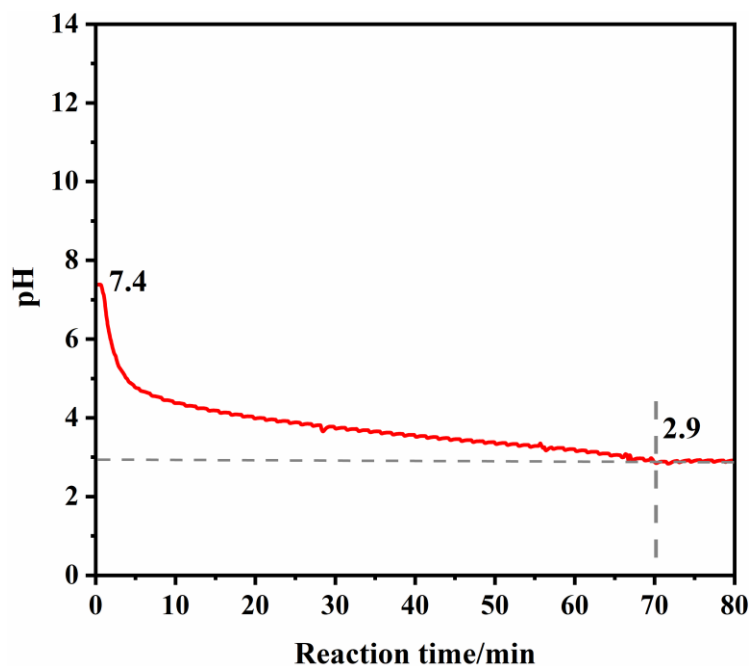


Figure S8. pH variation of the reaction system during isoeugenol ozonation.

Figure S9: Mid-infrared spectra of methyl vanillate, vanillic acid, vanillin and isoeugenol.

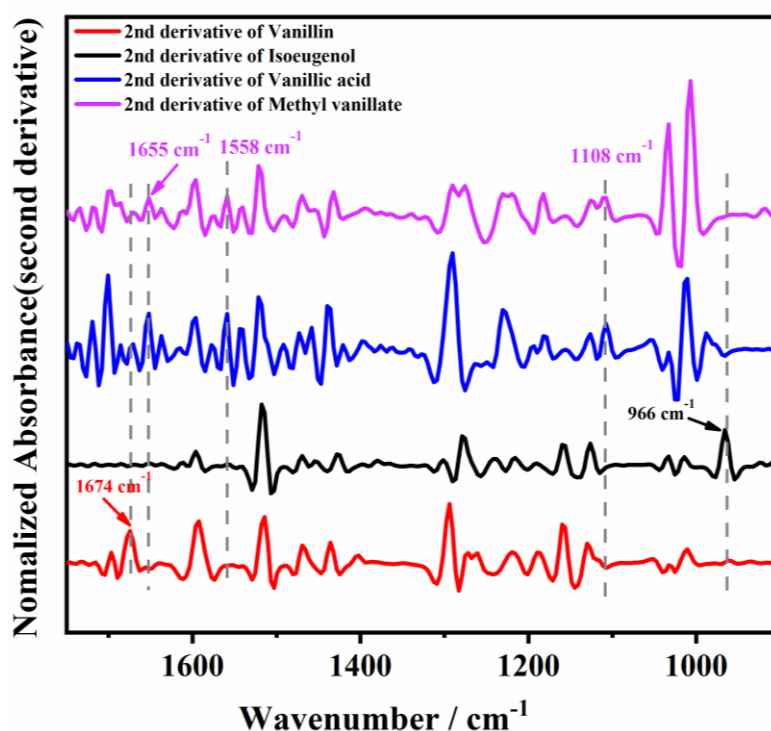


Figure S9. Mid-infrared spectra of methyl vanillate, vanillic acid vanillin and isoeugenol (second-order derivative spectra).

The relative calibration factor  $f$  for vanillic acid to vanillin and methyl vanillate to vanillin were calculated with the following equation:

$$f_{\text{vanillic acid}} = \frac{\varepsilon_{\text{vanillic acid}}}{\varepsilon_{\text{vanillin}}} = \frac{A_{\text{vanillic acid}}/A_{\text{vanillin}}}{c_{\text{vanillin}}/c_{\text{vanillic acid}}} = 0.2388 \quad (\text{equation S-2})$$

$$f_{\text{methyl vanillate}} = \frac{\varepsilon_{\text{methyl vanillate}}}{\varepsilon_{\text{vanillin}}} = \frac{A_{\text{methyl vanillate}}/A_{\text{vanillin}}}{c_{\text{vanillin}}/c_{\text{methyl vanillate}}} = 0.1469 \quad (\text{equation S-3})$$

Therefore, the vanillin yield pointed out by IR at the reaction endpoint was suggested to be corrected with the following equation:

$$\text{vanillin yield corrected\%} = \text{apparent yield\%} \times \frac{f_{\text{vanillin}} \cdot c_{\text{vanillin, endpoint}}}{f_{\text{vanillic acid}} \cdot c_{\text{vanillic acid, endpoint}} + f_{\text{methyl vanillate}} \cdot c_{\text{methyl vanillate, endpoint}} + f_{\text{vanillin}} \cdot c_{\text{vanillin, endpoint}}}, \text{ where } f_{\text{vanillin}} = 1$$

(equation S-4)

$$\text{vanillin yield corrected\%} = 96.99\% \times \frac{1 \times 86.98}{0.2388 \times 0.2794 + 0.1469 \times 0.2871 + 1 \times 86.98} = 96.86\%$$

**Figure S10: HPLC graphs during reaction and chromatogram for vanillic acid and methyl vanillate standard.**

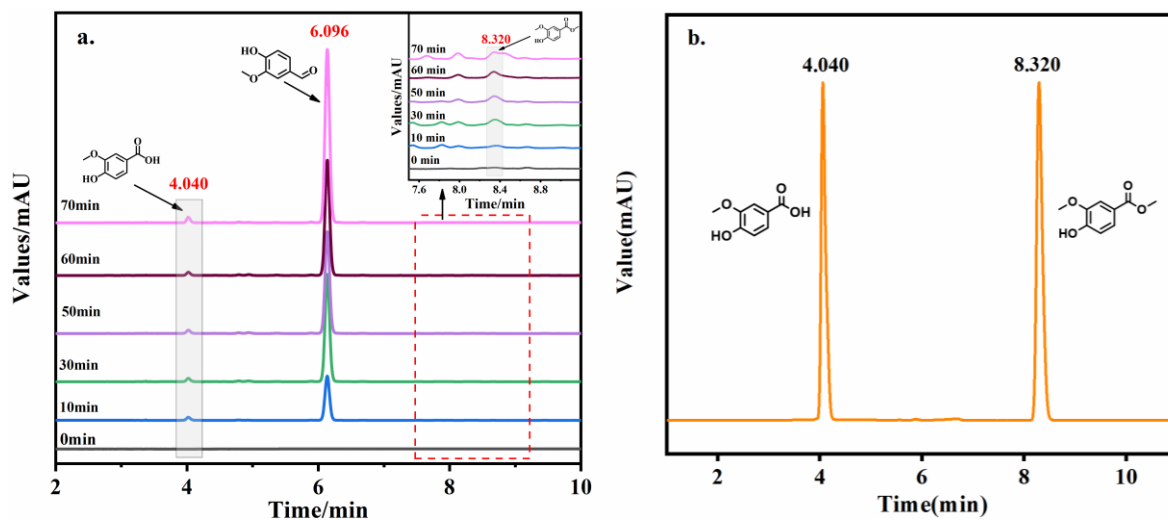
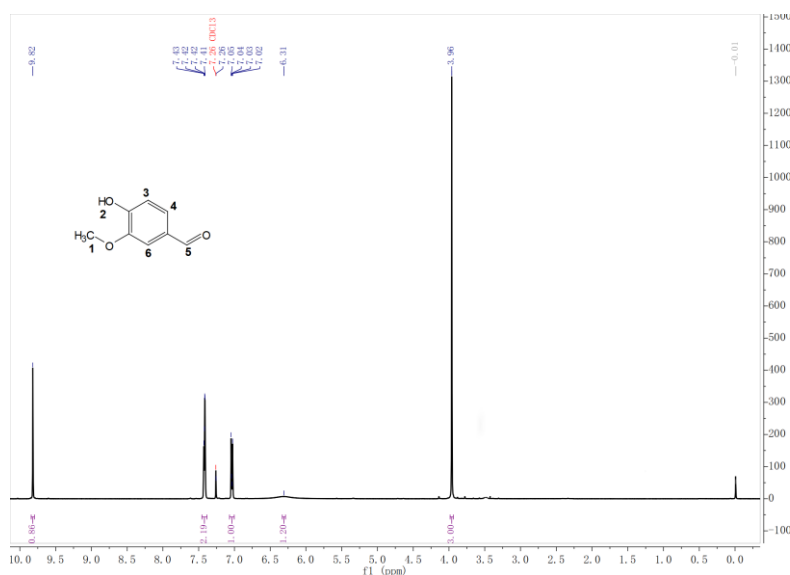


Figure S10. HPLC graph for (a) reaction system (inset was the enlarged region of the side products); (b) vanillic acid and methyl vanillate standard.

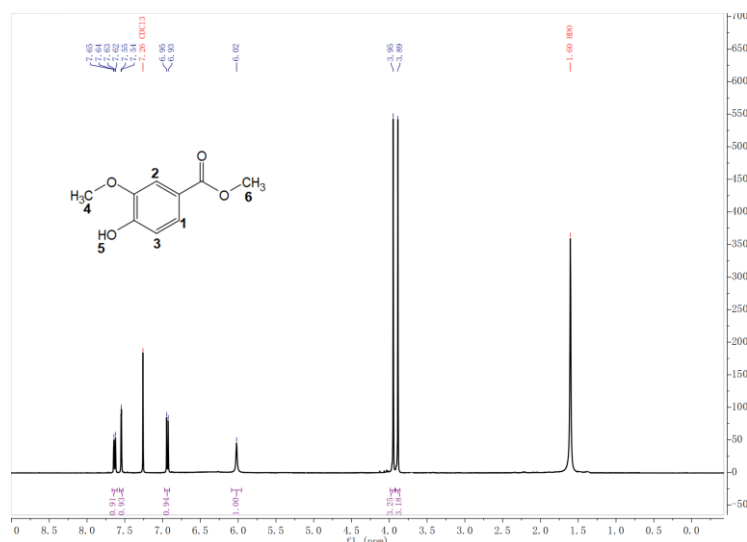
The relative calibration factor  $f$  for vanillic acid and methyl vanillate was calculated with the following equation:

$$f = \frac{m_{\text{vanillic acid}}/A_{\text{vanillic acid}}}{m_{\text{methyl vanillate}}/A_{\text{methyl vanillate}}} = 0.6329$$

**Figure S11:  $^1\text{H}$  NMR data for vanillin (product) and methyl vanillate (by product).**



The resolved data for hydrogen spectrum of vanillin (product) obtained as follows:  $\delta$  9.82 (s, 1H, -CHO), 7.42 (dd,  $J = 4.1, 2.4$  Hz, 2H, -C<sub>4</sub>H, -C<sub>6</sub>H), 7.04 (d,  $J = 8.6$  Hz, 1H, -C<sub>3</sub>H), 6.31 (s, 1H, -OH), 3.96 (s, 1H, -CH<sub>3</sub>).



The resolved data for hydrogen spectrum of methyl vanillate (by product) obtained as follows:  $\delta$  7.64 (dd,  $J = 8.3, 1.9$  Hz, 1H, -C<sub>1</sub>H), 7.55 (d,  $J = 1.9$  Hz, 1H, -C<sub>2</sub>H), 6.94 (d,  $J = 8.3$  Hz, 1H, -C<sub>3</sub>H), 6.02 (s, 1H, -OH), 3.95 (s, 3H, -C<sub>4</sub>H<sub>3</sub>), 3.89 (s, 3H, -C<sub>6</sub>H<sub>3</sub>).

Figure S11: <sup>1</sup>H NMR data for vanillin (product) and methyl vanillate (by product).

**Table S1 Characteristic peaks attributions for isoeugenol and vanillin.**

Table S1. Characteristic peaks attributions for isoeugenol and vanillin

Substances	Absorption Peak Position /cm <sup>-1</sup>	Peak Attribution	Reference
Isoeugenol	1594	Benzene ring backbone vibration	2, 3
	1515		
	1292	Bending vibration of the hydroxyl group	4, 3
	1275		
	1159	C-O stretching vibration	3
966	Stretching vibrations of olefinic C=C bond double substitution ( <i>trans</i> -)	4	
Vanillin	1674	Stretching vibrations of the C=O bond of the aldehyde group	2, 3
	1592	Benzene ring backbone vibration	2, 3
	1515		
	1294	Bending vibration of the hydroxyl group	3, 4
	1274		
1159	C-O stretching vibration	3	

**Table S2: Effect of gas flux of ozone generator on vanillin**Table S2. Effect of gas flux of ozone generator on vanillin selectivity<sup>a</sup>

Serial number	Gas Flux (L/min)	Reaction Time (min)	Isoeugenol conversion (%)	Vanillin Selectivity (%)
1	1.4	50	100	92.97±0.34
2	1.6	60	100	96.99±0.38
3	1.8	64	100	96.23±0.27
4	2	65	100	95.80±0.41
5	2.2	68	100	95.18±0.28

note:

<sup>a</sup> Experimental conditions: Isoeugenol concentration: 100 mg/mL,  $V_{\text{methanol}}: V_{\text{H}_2\text{O}}=85:15$ , Reaction temperature: 263.15 K.

**Table S3: Saturated solubility of vanillin in methanol-water system and pure water system.**

Table S3a. Saturated solubility of vanillin in methanol-water system at 258.15 K

Material in Solution	Serial Number	Volume Ratio of Water to Solvent Mixture (%)	Saturated Solubility
Vanillin	1	25	0.0244
	2	20	0.0265
	3	15	0.0304

Table S3b. Saturated solubility of vanillin and isoeugenol in pure water system at 278.15 K

Material in Solution	Solvent	Saturated Solubility
Vanillin	Water	$1.06 \times 10^{-4}$
Isoeugenol	Water	$3.29 \times 10^{-5}$

**Table S4: Effect of water content on vanillin yield**Table S4. Effect of water content on vanillin selectivity<sup>a</sup>

Serial Number	Volume Ratio of Water to Solvent Mixture (%)	Isoeugenol conversion (%)	Vanillin Selectivity (%)
1	20	100	90.64±0.46
2	15	100	96.99±0.40
3	10	100	92.39±0.27
4	5	100	91.02±0.39
5	1	100	71.36±0.38

note:

<sup>a</sup> Experimental conditions: Isoeugenol concentration: 100 mg/mL, gas flux: 1.6 L/min, Reaction temperature: 263.15 K.

**Table S5: Flash point of methanol-water system.**

Table S5. Flash point of methanol-water system

Volume Ratio of Water to Solvent Mixture / %	Open Flash Point in Air (without O <sub>3</sub> ) / K	Open Flash Point with O <sub>3</sub> / K
40	306.15±0.4	305.75±0.4
30	301.75±0.3	300.55±0.4
20	300.65±0.3	299.05±0.3
15	297.55±0.4	296.65±0.3
12.5	295.65±0.2	296.00±0.1
10	294.65±0.1	295.35±0.2

**Table S6: Effect of temperature on vanillin yield**Table S6. Effect of temperature on vanillin selectivity<sup>a</sup>

Serial Number	Temperature of Reaction (K)	Vanillin Selectivity (%)
1	268.15	92.57±0.39
2	265.65	92.93±0.41
3	263.15	96.99±0.32
4	260.65	94.66±0.40
5	258.15	90.47±0.36

<sup>a</sup> Experimental conditions: Gas flux: 1.6 L /min, Isoeugenol concentration: 100 mg/mL,  $V_{\text{methanol}}: V_{\text{H}_2\text{O}}=85:15$ .

**Table S7: Comparison of our work and previous studies (mostly) in recent 10 years for the preparation of vanillin from isoeugenol and eugenol**

Materials	Product	Reaction conditions	Solvent	Oxidant	Conversion	Selectivity
Isoeugenol <sup>5</sup>	Vanillin	HMF/FeMo (Catalyst), 80 °C, 24 h	No solvents	tertiary-butyl hydroperoxide	86%	83%
Isoeugenol <sup>6</sup>	Vanillin	CuOx/rGO carbocatalyst (Catalyst), 4 bar O <sub>2</sub> , 50 °C, 24 h	/	O <sub>2</sub>	97%	54%
Isoeugenol <sup>7</sup>	Vanillin	CeMCM-22 (Catalyst), 60 °C, 90 min	No solvents	H <sub>2</sub> O <sub>2</sub>	63%	75%
Isoeugenol <sup>8</sup>	Vanillin	Fe-SBA15-HSO <sub>3</sub> <sup>BM-IM</sup> (Catalyst), 90 °C, 1 h	acetonitrile	H <sub>2</sub> O <sub>2</sub>	93%	50%
Isoeugenol <sup>9</sup>	Vanillin	humins-containing Fe <sub>2</sub> O <sub>3</sub> (Catalyst), 15 bar, 100 °C, 100 min	acetonitrile	H <sub>2</sub> O <sub>2</sub>	40%	45%
Isoeugenol <sup>10</sup>	Vanillin	1% Fe/RGO (Catalyst), 90 °C, 2 h	acetonitrile	H <sub>2</sub> O <sub>2</sub>	61%	63%
Isoeugenol <sup>11</sup>	Vanillin	Cu-MINT (Catalyst), 80 °C, 6 h	acetonitrile	H <sub>2</sub> O <sub>2</sub>	58%	88%
Isoeugenol <sup>12</sup>	Vanillin	0.5Nb/Al-SBA-15 (Catalyst), 90 °C, 2 h	acetonitrile	H <sub>2</sub> O <sub>2</sub>	69%	66%
Isoeugenol <sup>13</sup>	Vanillin	CuO/MgAl <sub>2</sub> O <sub>4</sub> (Catalyst), 90 °C, 8 h	acetonitrile	H <sub>2</sub> O <sub>2</sub>	81%	100%
Isoeugenol <sup>14</sup>	Vanillin	sewage sludgederived biomaterial (Catalyst), 90 °C, 1 h	acetonitrile	H <sub>2</sub> O <sub>2</sub>	80%	65%
Isoeugenol <sup>15</sup>	Vanillin	FeMag-190 (Catalyst), 90 °C, 24 h	acetonitrile	H <sub>2</sub> O <sub>2</sub>	85%	57%
Isoeugenol <sup>16</sup>	Vanillin	Ir <sub>1</sub> Cu <sub>1</sub> -In <sub>2</sub> O <sub>3</sub> (Catalyst), 2 bar O <sub>2</sub> , 70 °C, 2 h	acetonitrile	O <sub>2</sub>	/	90.5%
Eugenol <sup>17</sup>	Vanillin	Co(OAc) <sub>2</sub> • 4H <sub>2</sub> O (Catalyst), 80 °C, 5.0 equiv NaOH 0.5 atm O <sub>2</sub> , 20 h	methanol	O <sub>2</sub>	100%	68.5%
Isoeugenol <sup>18</sup>	Vanillin	0 °C	EtOAc-H <sub>2</sub> O	O <sub>3</sub>	/	49%
The present work		-10 °C, 1 h	methanol	O <sub>3</sub>	100%	96.86%

**Table S8: Criteria for assessing the severity of runaway reaction based on  $\Delta T_{ad}$** Table S8. Criteria for assessing the severity of runaway reaction<sup>19</sup>

Level	$\Delta T_{ad}/K$	Consequence
1	$\Delta T_{ad} \leq 50$ , without pressure influence	When there is no danger of pressure increase due to gas, there will be loss of material in a single batch.
2	$50 < \Delta T_{ad} < 200$	Plant damage.
3	$200 \leq \Delta T_{ad} < 400$	The rise of temperature leads to the rise of the reaction rate, and once the reaction is out of control, the system temperature will change dramatically in a short time, resulting in serious losses in the plant.
4	$\Delta T_{ad} \geq 400$	The rise of temperature leads to the rise of the reaction rate, and once the reaction is out of control, the system temperature will change dramatically in a short time, causing devastating losses in the factory.

**Reference**

1. Y. Wan, P. Zhang, H. He, J. Sha, K. Yang, T. Li and B. Ren, *Journal of Chemical & Engineering Data*, 2019, **64**, 5142-5159.
2. A. Vizintin, J. Bitenc, A. Kopac Lautar, J. Grdadolnik, A. Randon Vitanova and K. Pirnat, *ChemSusChem*, 2020, **13**, 2328-2336.
3. A. R. Kumar, S. Selvaraj, K. S. Jayaprakash, S. Gunasekaran, S. Kumaresan, J. Devanathan, K. A. Selvam, L. Ramadass, M. Mani and P. Rajkumar, *Journal of Molecular Structure*, 2021, **1229**, 129490.
4. S. Olsztynska-Janus and M. A. Czarnecki, *Spectrochim Acta A Mol Biomol Spectrosc*, 2020, **238**, 118436.
5. P. P. Neethu, A. Sreenavva and A. Sakthivel, *Applied Catalysis A: General*, 2021, **623**, 118292.
6. A. Bohre, D. Gupta, M. I. Alam, R. K. Sharma and B. Saha, *ChemistrySelect*, 2017, **2**, 3129-3136.
7. P. Sahu, V. Ganesh and A. Sakthivel, *Catalysis Communications*, 2020, **145**, 106099.
8. S. Ostovar, A. Franco, A. R. Puente-Santiago, M. Pinilla-de Dios, D. Rodriguez-Padron, H. R. Shaterian and R. Luque, *Front Chem*, 2018, **6**, 77-84.
9. L. Filicetto, M. D. Márquez-Medina, A. Pineda, A. M. Balu, A. A. Romero, C. Angelici, E. de Jong, J. C. van der Waal and R. Luque, *Catalysis Today*, 2021, **368**, 281-290.
10. A. Franco, S. De, A. M. Balu, A. Garcia and R. Luque, *Beilstein J Org Chem*, 2017, **13**, 1439-1445.
11. P. García-Albar, N. Lázaro, Z. A. Alothman, A. A. Romero, R. Luque and A. Pineda, *Molecular Catalysis*, 2021, **506**, 111537.
12. A. Franco, S. De, A. M. Balu, A. A. Romero and R. Luque, *ChemistrySelect*, 2017, **2**, 9546-9551.
13. B. Rahmanivahid, M. Pinilla-de Dios, M. Haghghi and R. Luque, *Molecules*, 2019, **24**, 2597-2615.
14. A. Franco, J. Fernandes de Souza, P. F. Pinheiro do Nascimento, M. Mendes Pedroza, L. S. de Carvalho, E. Rodriguez-Castellón and R. Luque, *ACS Sustainable Chemistry & Engineering*, 2019, **7**, 7519-7526.
15. M. D. Marquez-Medina, P. Prinsen, H. Li, K. Shih, A. A. Romero and R. Luque, *ChemSusChem*, 2018, **11**, 389-396.
16. X. Zhao, R. Fang, F. Wang, X.-P. Kong and Y. Li, *ACS Catalysis*, 2022, **12**, 8503-8510.
17. H. Mao, L. Wang, F. Zhao, J. Wu, H. Huo and J. Yu, *Journal of the Chinese Chemical Society*, 2016, **63**, 261-266.
18. A. J. Kendall, J. T. Barry, D. T. Seidenkranz, A. Ryerson, C. Hiatt, C. A. Salazar, D. J. Bryant and D. R. Tyler, *Tetrahedron Letters*, 2016, **57**, 1342-1345.
19. Specification for safety risk assessment of fine chemical reactions[S]. *GB/T42300-2022*, 2022.